Molecular Biology of the Cell
Vol. 21, 2649–2660, August 1, 2010

Epigenetic Modification Affecting Expression of Cell Polarity and Cell Fate Genes to Regulate Lineage Specification in the Early Mouse Embryo

David-Emlyn Parfitt*† and Magdalena Zernicka-Goetz*†

*Wellcome Trust/CR UK Gurdon Institute, Cambridge CB2 1QN, United Kingdom; and †Department of Physiology, Development and Neuroscience, University of Cambridge, Cambridge CB2 3DY, United Kingdom

Submitted January 21, 2010; Revised April 21, 2010; Accepted June 3, 2010
Monitoring Editor: Benjamin Margolis

Formation of inner and outer cells of the mouse embryo distinguishes pluripotent inner cell mass (ICM) from differentiating trophectoderm (TE). Carm1, which methylates histone H3R17 and R26, directs cells to ICM rather that TE. To understand the mechanism by which this epigenetic modification directs cell fate, we generated embryos with in vivo–labeled cells of different Carm1 levels, using time-lapse imaging to reveal dynamics of their behavior, and related this to cell polarization. This shows that Carm1 affects cell fate by promoting asymmetric divisions, that direct one daughter cell inside, and cell engulfment, where neighboring cells with lower Carm1 levels compete for outside positions. This is associated with changes to the expression pattern and spatial distribution of cell polarity proteins: Cells with higher Carm1 levels show reduced expression and apical localization of Par3 and a dramatic increase in expression of PKCII, antagonist of the apical protein aPKC. Expression and basolateral localization of the mouse Par1 homologue, EMK1, increases concomitantly. Increased Carm1 also reduces Cdx2 expression, a transcription factor key for TE differentiation. These results demonstrate how the extent of a specific epigenetic modification could affect expression of cell polarity and fate-determining genes to ensure lineage allocation in the mouse embryo.

INTRODUCTION

The first 3 d of mouse development involve the transition from a single cell, the zygote, to the blastocyst, which consists of a group of pluripotent cells destined to form the embryo proper (inner cell mass [ICM]) surrounded by trophectoderm (TE), whose derivatives form structures such as the placenta. The precise mechanism governing the allocation of cells to inner and outer positions, to form ICM and TE, respectively, remains unclear.

Epigenetic mechanisms are thought likely to be involved in cell lineage allocation and specification (Shi and Wu, 2009). The posttranslational modification of histone (H) proteins regulate the spatiotemporal expression patterns of genes by altering chromatin structure, restricting or facilitating access for transcription factors that control gene expression. Consequently, varying levels of particular modifications can be associated with particular cell types. For example, the methylation of H3K9me3 and H3K27me3 is associated with the suppression of differentiation-associated genes, and levels of these modifications are higher in ICM cells than TE (Erhardt *et al.*, 2003). In contrast, H3K4me3 and acetylated H4K16 are markers of transcriptional activity and tend to be associated with the expression of pluripotency related genes *Nanog*, *Sox2*, and *Oct4/Pou5f* in ICM cells (O'Neill *et al.*, 2006). A role for epigenetic modification in the allocation of cells to the different blastocyst lineages was first suggested by the observation that the levels of H3R26me2 and H3R17me2 varied in four-cell stage blastomeres according to their expected fate (Torres-Padilla *et al.*, 2007). Specifically, H3R26me2 levels were found to be lowest in blastomeres contributing more to the TE surrounding the blastocyst cavity and highest in blastomeres contributing significantly more cells to the ICM and its surrounding polar TE (Piotrowska-Nitsche *et al.*, 2005; Torres-Padilla *et al.*, 2007). The enzyme that mediates the transfer of methyl groups to arginine residues, including H3R26, is Carm1 (Chen *et al.*, 1999; Schurter *et al.*, 2001). Elevated expression of Carm1 leads blastomeres to preferentially contribute to the ICM (Torres-Padilla *et al.*, 2007), indicating that this particular epigenetic modification may be driving blastomeres to a particular fate. The mechanism whereby blastomeres with higher levels of H3R26/R17me2 contribute to the ICM and those with lower H3R26/R17me2 levels to TE lineages and whether such differences could culminate in altered expression of particular genes that direct cell allocation and lineage determination, have remained unknown.

Inner and outer cell allocation is largely directed by particular blastomere division orientations at the 8–16- and 16–32-cell transitions (Barlow *et al.*, 1972; Johnson and Ziomek, 1981a,b; Pedersen *et al.*, 1986; Dyce *et al.*, 1987; Fleming, 1987). Divisions that generate two outside cells are described as symmetric and those generating one outside and one inside cell, asymmetric. The ratio of asymmetric and symmetric divisions and their spatial and temporal regionalization can therefore serve to regulate cell contributions to the ICM and TE (Fleming, 1987; Plusa *et al.*, 2005; Bischoff *et al.*, 2008; Jedrusik *et al.*, 2008; for review Zernicka-Goetz *et al.*,

This article was published online ahead of print in *MBoC in Press* (http://www.molbiolcell.org/cgi/doi/10.1091/mbc.E10–01–0053) on June 16, 2010.

Address correspondence to: Magdalena Zernicka-Goetz (mzg@mole.bio.cam.ac.uk).

2009). Such divisions are preceded by apical–basal blastomere polarization, which facilitates the generation of phenotypically distinct daughter cells from asymmetric divisions: the outer cells are polar and inner cells, apolar (Johnson and Ziomek, 1981a,b; Houliston *et al.*, 1989). Symmetric division, on the other the hand, gives rise to two outer cells that are phenotypically similar. Conserved cell polarity molecules such as Par3, atypical protein kinase C (aPKC), Jam1, and Par6 are key for setting up polarity in many model systems (Goldstein and Macara, 2007). These molecules localize apically during polarization of eight-cell blastomeres of the mouse embryo (Thomas *et al.*, 2004; Plusa *et al.*, 2005; Vinot *et al.*, 2005). Moreover, their down-regulation leads cells to preferentially adopt inside positions and develop into ICM (Plusa *et al.*, 2005). Accordingly, depletion of aPKCλ demonstrated that it is required for symmetric division in *Xenopus* embryos (Nakaya *et al.*, 2000). More recent studies have revealed that the TE-specific transcription factor Cdx2 (Niwa *et al.*, 2005) also contributes to whether cells divide symmetrically or asymmetrically, through effects on the degree of cell polarization (Jedrusik *et al.*, 2008). Up-regulation of Cdx2 was associated with promoted apical localization of aPKCζ, symmetric division and, consequently, an increased contribution to the TE. However, none of the studies carried out to date have shown how some epigenetic modification can mediate cell lineage allocation in the early mouse embryos.

Here we provide evidence that the expression levels of Carm1 in individual blastomeres of the mouse embryo affects cell polarity and, thus, cell fate. We show that increasing levels of Carm1 alters the expression patterns of cell polarity genes such as Par3, EMK1, aPKCζ, and PKCII and the transcription factor Cdx2, which regulates the transition away from pluripotency. These changes are associated with cells being internalized, both by asymmetric divisions and as a result of being engulfed by neighboring cells competing for outside positions. These results lead us to propose a model in which the extent of a particular epigenetic modification affects the expression levels of key cell polarity and fate determining genes to regulate inner versus outer cell allocation and lineage determination during development of the preimplantation mouse embryo.

MATERIALS AND METHODS

Embryo Collection and Culture

Embryos were collected into M2 medium (+4 mg/ml BSA) from superovulated C57Bl6xCBA females mated with C57Bl6xCBA or H2B-EGFP (Hadjantonakis and Papaioannou, 2004) males as described before (Bischoff *et al.*, 2008). Embryos were cultured in KSOM (+4 mg/ml BSA) under paraffin oil in 5% CO_2 at 37.5°C.

mRNA Microinjection

mRNAs were transcribed in vitro using mMessage mMachine T3 polymerase (Ambion, Austin, TX) from linearized pRN3P vector containing the following constructs: Carm1.HA (full-length Carm1-coding sequence with a C-terminal hemagglutinin [HA] tag; Chen *et al.*, 1999), Carm1(E267Q).HA (as Carm1.HA, but with an E267Q mutation generated with the QuickChange site-directed mutagenesis kit; Stratagene, La Jolla, CA; Lee *et al.*, 2002) and DsRed. RNA was diluted in RNase-free H_2O and working concentrations were as follows: *Carm1.HA* and *Carm1(E267Q).HA*, 0.8–1.0 μg/μl; dsRed 0.05 μg/μl. All microinjections were carried out as previously described (Zernicka-Goetz *et al.*, 1997).

Time-Lapse Imaging and Analysis

Fluorescence and DIC Z-stacks of embryos from the zygote (24 h after human chorionic gonadotropin [hCG]) or two-cell (44 h after hCG) to blastocyst stage were collected on 15 focal planes every 15 min for ~96 and 72 h of continuous embryo culture, respectively. The images were processed as described previously (Bischoff *et al.*, 2008). All cells were followed in 4D using SIMI Biocell software (http://www.simi.com/en/products/biocell/index.html/; Schnabel *et al.*, 1997): The 3D coordinates of every nucleus were taken every 2–3 frames, including one frame before and one after cell cleavages. Between each of these "fixed" points, cell movement was intercalated by SIMI Biocell software. Cell behavior was defined using the position of daughter cells shortly after mitosis and at the end of their cell cycle to determine whether they had moved from or toward the outside, as in our previous study (Bischoff *et al.*, 2008). If the DIC images indicated a cell with a clear outside surface (e.g., highlighted in Figure 2) and if there were no surrounding nuclei in the fluorescence images, including consideration for nuclei above or below in the z-plane, then a cell was defined as outer and vice versa for cells that did not meet these criteria. By following every cell in the recording and using the DsRed fluorescence signal at the two-cell stage to determine which blastomere had been injected with *Carm1* or *Carm1(E267Q)* mRNA, complete lineages of the behavior of all cells up to the blastocyst stage were generated. This dataset allowed the position, fate allocation and division orientation of all cells to be determined individually.

Immunofluorescence Staining

Immunofluorescence staining was carried out as in Jedrusik *et al.* (2008). Primary antibodies used were as follows: Cdx2 mouse monoclonal (BioGenex, San Ramon, CA), 1:200 in PBS-Tween containing 3% wt/vol BSA; aPKCζ rabbit polyclonal (Santa Cruz Biotechnology, Santa Cruz, CA), 1:200; H3 dimethyl R26 rabbit polyclonal (Abcam, Cambridge, MA), 1:150; Carm1 rabbit polyclonal (Jackson ImmunoResearch Laboratories, West Grove, PA), 1:200; Par3 rabbit polyclonal (Millipore, Bedford, MA) 1:50; EMK1 rabbit polyclonal (Hurov *et al.*, 2004), 1:150. Secondary antibodies used were AlexaFluor 488–conjugated anti-mouse (Jackson ImmunoResearch Laboratories) and AlexaFluor 488–conjugated anti-rabbit (Invitrogen, Carlsbad, CA), both at 1:500.

For the time course of aPKCζ expression, embryos were collected 40 h after hCG (midlate two-cell), cultured in KSOM and checked 3–4 times per day for their progression. Embryos were fixed at mid-four-cell (approx. 50 h after hCG), mid-eight-cell (6–7 h after 4–8-cell division), mid-16-cell (75 h after hCG), and early blastocyst stages (82 h after hCG) and immunostained as above. Confocal microscopy was performed using a 63×/1.4 NA oil DIC Plan-Apochromat lens on an upright Zeiss 510 Meta confocal microscope (Thornwood, NY). Confocal sections were taken every 2 μm through the whole embryo and, where appropriate, the fluorescence signal was projected using ImageJ software (http://rsb.info.nih.gov/ij/). To objectively measure the fluorescence levels of proteins, individual cells were outlined manually in Image J, and the intensity of the fluorescent signal was recorded for each z-stack (on average, 7.4 per cell). These values were normalized against those measured for DAPI (on average, 3.3 measurements per nucleus) and averaged for each population of injected and noninjected cells in both experimental (*Carm1*-injected) and control [*Carm1(E267Q)*-injected] embryos.

Quantitative RT-PCR

To investigate gene expression after *Carm1* or *Carm1(E267Q)* mRNA injection, 25 embryos in which *Carm1* or *Carm1(E267Q)* mRNAs were injected with that of *DsRed* into one two-cell blastomere were disaggregated 6–7 h after blastomere division to the eight-cell stage: Zonae were removed with 0.5% pronase in PBS, the embryos were incubated in Ca^{2+}/Mg^{2+}-free M2 for 3–5 min, separated into 2/8 blastomere pairs or 1/8 singlets by pipetting, and segregated into groups based on the presence/absence of DsRed. For each of three biological replicates, the 100 red and 100 non-red blastomeres collected were placed into 10 μl of RNA extraction buffer and snap-frozen until used in quantitative RT-PCR (qRT-PCR). For time-course experiments, 50 zygotes, early, mid, and late two-cell (approx. 18, 28, 34, and 40 h after hCG), early and late four-cell (approx. 46 and 54 h after hCG), early, mid and late eight-cell (4, 7, or 10 h after eight-cell onset), early and late 16-cell embryos (4 and 10 h after 16-cell onset), and early blastocysts were used for RNA extraction and qRT-PCR. For all samples, PicoPure RNA isolation kits (Arcturus Bioscience, Mountain View, CA) were used for RNA extraction; samples were DNase treated using the DNA-free kit (Ambion), and cDNA synthesis was performed using SuperScript III Reverse Transcriptase (Invitrogen), including $Oligo(dT)_{20}$ and RNaseOUT Recombinant RNase Inhibitor. Products were diluted 10-fold and 2 μl was used per PCR. Reactions were performed in technical triplicate for each primer pair (Supplemental Information) with SYBR Green Master Mix (Applied Biosystems, Foster City, CA) in optical 96-well reaction plates on an AbiPrism 7000 Sequence Detection System. Analysis and statistics were calculated in Excel (Microsoft, Redmond, WA), and all normalization done against *ActB* expression using the following equation: $2^{(Ct(ActB) - Ct(gene\ x))}$.

RESULTS

Carm1 Elevation Affects the Ratio of Asymmetric to Symmetric Blastomere Divisions

Increased levels of Carm1 were reported to lead cells to contribute preferentially to the ICM rather than TE lineage

in mouse embryos (Torres-Padilla *et al.*, 2007), but the mechanism behind the effect of Carm1 on lineage allocation remained unknown. To address this question, we microinjected synthetic mRNA for either *Carm1* or *Carm1*(*E267Q*), which encodes an enzymatically inactive protein (Lee *et al.*, 2002; Torres-Padilla *et al.*, 2007), into one late two-cell blastomere to up-regulate Carm1 in just half of the embryo. To identify this half, in all experiments *DsRed* mRNA was coinjected as a lineage marker. This approach led, on average, to a 5.0-fold increase in the level of Carm1 transcript in the progeny of *Carm1* injected cells in comparison to their noninjected counterparts. The overexpression of Carm1 was also confirmed on the protein level (Supplemental Figure 1). To understand how cells with higher Carm1 levels can change their lineage allocation versus cells with lower levels of Carm1, we used a live-imaging approach that allowed us to track the positions and division orientations of all cells in embryos as they develop to the blastocyst stage. To enable a direct comparison of the cell behavior in these embryos with that of previously reported unmanipulated, wild-type embryos, we used the same methods of imaging and analysis as established previously (Bischoff *et al.*, 2008). DIC and fluorescence sections were recorded on 15 focal planes at each time point every 15 min for ~72 h, during development from the two-cell to blastocyst stages. Embryos were derived from a H2B-enhanced green fluorescent protein (EGFP) transgenic reporter line, which allowed visualization of their nuclei via fluorescent chromatin.

We found that 88% ($n = 26$, three independent experiments) of embryos in our time-lapse recordings reached the blastocyst stage, and all cells could be tracked in 61% ($n = 14$) of these embryos (the remaining seven embryos either showed too weak an EGFP signal to confidently determine the position of all their cells, or they moved from the field of view during recordings). Similarly, in *Carm1(E267Q)* injected control groups, the great majority (93%, $n = 31$, three independent experiments) of imaged embryos reached the blastocyst stage, and all cells could be tracked in 12 of them (as before, the remaining embryos were either not in the field of view throughout imaging, or the EGFP signal was too weak to track their cells. One embryo was eliminated as it was asynchronous with other embryos imaged, reaching 46 cells before any of the others developed to the blastocyst stage).

After imaging, the total number of cells per embryo in the *Carm1* group was, on average, 31.5 (±1.0), of which 19.2 (±4.9) were outer (TE) and 12.2 (±4.9) were inner (ICM) cells. The number of cells derived from the *Carm1*-injected clone was similar to that derived from the noninjected clone (Figure 1A). However, when we analyzed the contribution of individual cells to the ICM, we found that the significant majority (74.9%) were derived from the blastomere in which the Carm1 level was increased (Figure 1A). The opposite was true when we analyzed the contribution of clones to the TE. The proportion of outer cells derived from blastomeres with artificially higher levels of Carm1 was on average 35.4%; thus, the significant majority (64.6%) of the TE was derived from the clone in which Carm1 levels remained unchanged. This tendency was not observed when *Carm1(E267Q)* mRNA was overexpressed in place of Carm1: approximately half (47.8%) the progeny of the *Carm1(E267Q)*-injected blastomere contributed to the ICM and half (52.2%) to the TE (Figure 1B). Thus, elevated expression of Carm1 in a two-cell blastomere leads its progeny to contribute predominantly to the ICM (Student's *t* test, $p = 0.00022$), in agreement with previous studies (Torres-Padilla *et al.*, 2007).

To understand whether differences in cell dynamics between the *Carm1*-injected and noninjected cells within the same embryo accounted for the former's more extensive ICM allocation, we analyzed the behavior of all cells in 4D, until their allocation to the ICM and TE at the early blastocyst stage. Inner cells are largely generated through asymmetric division of eight- and 16-cell blastomeres and the division of inside cells from the 16-cell stage. To assess whether Carm1 up-regulation was associated with a change in the proportion of asymmetric/symmetric divisions, we used Simi Biocell reconstructions to determine the division orientation of the progeny of both two-cell blastomeres. These were classified by scoring the positions of daughter cells relative to each other and to the embryo surface one frame before and one after their mitotic division in both DIC and fluorescence images. This allowed the direct comparison of the proportions of asymmetric/symmetric divisions between *Carm1*/*Carm1(E267Q)*-injected and noninjected clones (Figure 1C, Supplemental Movie).

We found that during the 4th cleavage, the clone of cells in which Carm1 levels were up-regulated took more asymmetric divisions in comparison to the noninjected clone (on average, 60.0 and 52.8%, respectively ($p = 0.0007$; Figure 1D). Similarly, the proportion of asymmetric divisions taken by the *Carm1*-injected clone was higher than that of the *Carm1*(*E267Q*)-injected clone, which was 51.9% ($p = 0.0024$). In contrast, when we compared the proportion of asymmetric divisions between noninjected clones of *Carm1* and *Carm1(E267Q)* groups, we found them to be statistically equivalent (52.8 and 55.5%, respectively, $p = 0.43$). Similarly, the proportion of asymmetric divisions was statistically equal in *Carm1(E267Q)*-injected and noninjected blastomeres of the same embryos (52.3 and 55.1%, respectively; $p = 0.097$).

During 5th cleavage, we observed that the frequency of symmetric divisions was higher than asymmetric ones in the *Carm1*(*E267Q*)-injected clone (54.8 vs. 45.2%, respectively, $p < 0.001$) and the noninjected clone (54.6 vs. 45.4%, respectively, $p < 0.001$) in the same embryos, in accord with previous studies (Bischoff *et al.*, 2008; Jedrusik *et al.*, 2008). In contrast, cells with increased levels of Carm1 undertook significantly more asymmetric (61.1%) than symmetric (38.9%) divisions ($p < 0.001$) during this cleavage period. Indeed, the proportion of asymmetric divisions was significantly higher in cells with increased levels of Carm1 than in the noninjected clone of the same embryos (47.6%, $p < 0.001$) and in *Carm1*(*E267Q*)-injected clones (45.2%, $p < 0.001$). These results provide evidence that elevation of Carm1 leads cells to contribute more to the ICM through an increase in the proportion of asymmetric over symmetric divisions, in particular, during the 5th cleavage period.

Carm1 Leads to Cell Movement to the Inside Compartment of the Embryo

We wondered whether the observed tendency for cells with elevated Carm1 to contribute to the ICM resulted exclusively from an effect on division orientation. Previous time-lapse studies of intact, unmanipulated embryos demonstrated that cell movements from the outside to the inside compartment are rare, occurring in only 1.6% of all 16- and 32-cell blastomeres taken together ($n = 3168$, from 66 embryos; Bischoff *et al.*, 2008). Reanalysis of this published data shows that 22% (11/51) of these movements occurred during the 16-cell stage and in the majority of cases (7/11), they were from an inner to outer position rather than in the opposite direction. Of the 40 movements observed during

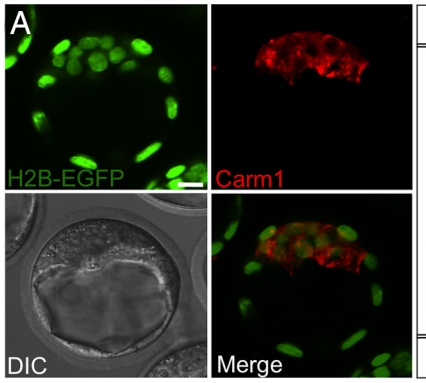

Embryo	No. of Cells	No. Red Cells (% of all cells)	No. Inner (% of Total)	Inner Carm1 +ive (% of inner)	No. Outer (% of total)	Outer Carm1 +ive (% of Outer)
Carm1 1	32	16 (50)	11 (34)	9 (82)	21 (66)	7 (33)
Carm1 2	30	16 (53)	10 (33)	8 (80)	20 (67)	8 (40)
Carm1 3	32	16 (50)	14 (44)	10 (71)	18 (56)	6 (33)
Carm1 4	32	16 (50)	13 (41)	8 (62)	19 (59)	8 (42)
Carm1 5	32	16 (50)	13 (41)	10 (77)	19 (59)	6 (32)
Carm1 6	32	16 (50)	11 (34)	9 (82)	21 (66)	7 (33)
Carm1 7	29	16 (55)	13 (45)	9 (69)	16 (45)	7 (44)
Carm1 8	31	15 (48)	15 (48)	10 (67)	16 (52)	5 (31)
Carm1 9	32	16 (50)	14 (44)	11 (79)	18 (56)	5 (28)
Carm1 10	32	16 (50)	12 (38)	8 (67)	20 (62)	8 (40)
Carm1 11	32	16 (50)	13 (41)	10 (77)	19 (59)	6 (32)
Carm1 12	32	16 (50)	11 (34)	8 (73)	21 (66)	8 (38)
Carm1 13	32	16 (50)	10 (31)	8 (80)	22 (69)	8 (38)
Carm1 14	32	16 (50)	12 (38)	10 (83)	20 (62)	6 (32)
MEAN	31.5	15.9 (50.4)	12.2 (39.0)	*9.1 (74.9)	19.2 (60.3)	^6.8(35.4)
SD	1.0	1.8	4.9	6.7	4.9	5.1

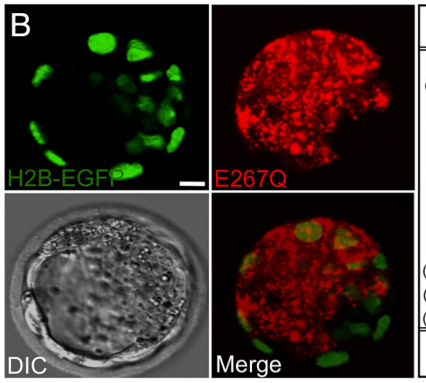

Embryo	No. of Cells	No. Red Cells (% of all cells)	No. Inner (% of total)	Inner E267Q +ive (% of inner)	No. Outer (% of total)	Outer E267Q +ive (% of Outer)
(E267Q) 1	31	15 (48)	12 (39)	4 (33)	19 (61)	11 (58)
(E267Q) 2	32	16 (50)	16 (50)	9 (56)	16 (50)	7 (44)
(E267Q) 3	31	16 (52)	11 (35)	5 (45)	20 (65)	11 (55)
(E267Q) 4	32	16 (50)	9 (38)	5 (56)	23 (72)	11 (48)
(E267Q) 5	32	16 (50)	11 (34)	5 (45)	21 (66)	11 (52)
(E267Q) 6	32	16 (50)	13 (41)	7 (54)	19 (59)	9 (47)
(E267Q) 7	32	16 (50)	13 (41)	6 (46)	19 (59)	10 (53)
(E267Q) 8	32	16 (50)	11 (34)	5 (45)	21 (66)	11 (52)
(E267Q) 9	32	16 (50)	15 (47)	8 (53)	17 (53)	8 (47)
(E267Q) 10	32	16 (50)	10 (31)	4 (40)	22 (69)	12 (55)
(E267Q) 11	32	16 (50)	11 (34)	4 (36)	21 (66)	12 (57)
(E267Q) 12	32	16 (50)	11 (34)	7 (64)	21 (66)	9 (43)
MEAN	31.8	15.9(50)	11.9 (38.2)	*5.8(47.8)	19.9 (61.8)	^9.5 (52.2)
SD	3.9	0.3	2.0	1.7	2.2	1.6

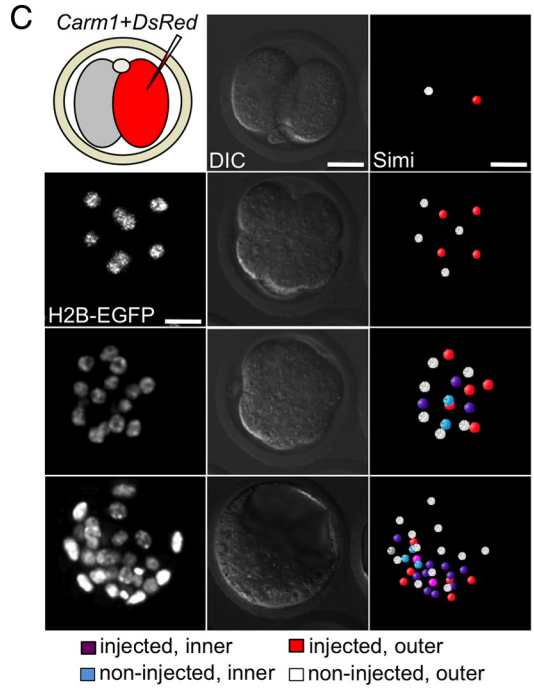

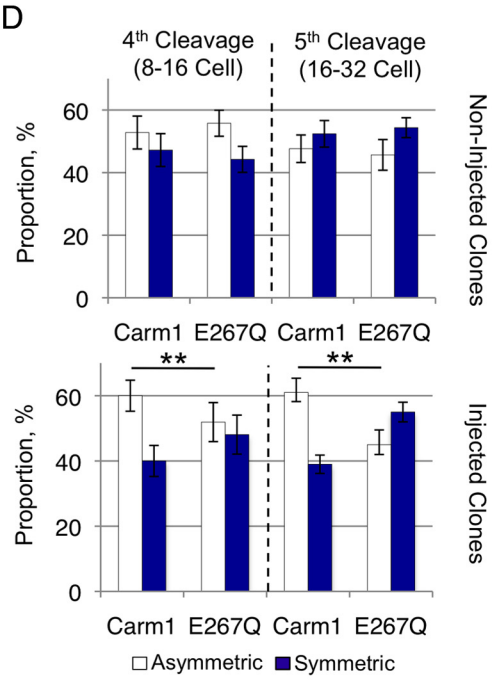

Figure 1. Carm1 increases blastomere contribution to the ICM and frequency of asymmetric division. two-cell blastomeres of H2B-EGFP embryos were injected with *Carm1* (A) or *Carm1(E267Q)* (B) and *DsRed* mRNAs. After time-lapse microscopy, cells were scored as inner/outer and DsRed positive and negative. Student's t tests: *p = 0.00022, ^ p = 0.00091. (C) H2B-EGFP–expressing embryos were injected as in A, time-lapse imaged to the blastocyst stage and tracked using Simi Biocell software. DIC and GFP Z-stack images were used to determine positions of blastomeres every 15 min. Examples where *Carm1+DsRed* mRNAs were injected are shown. (D) Average proportions of asymmetric and symmetric divisions during 4th and 5th cleavage for noninjected (top) and injected (bottom) clones in experimental (Carm1, n = 14) and control (E267Q, n = 12) embryos. Error bars, SEM. Student's t test: **p < 0.001. Scale bar, 10 μm.

the 32-cell stage, the majority (82.5%) were from an inner to an outer position.

To identify whether such cell repositioning happens after Carm1 up-regulation, we scored the position (inner or outer) of daughter cells both immediately after their mitotic division and at the end of their cell cycle, to check whether this had changed (Figure 2A; see *Materials and Methods*). This revealed that in control, *Carm1(E267Q)* embryos, cell move-

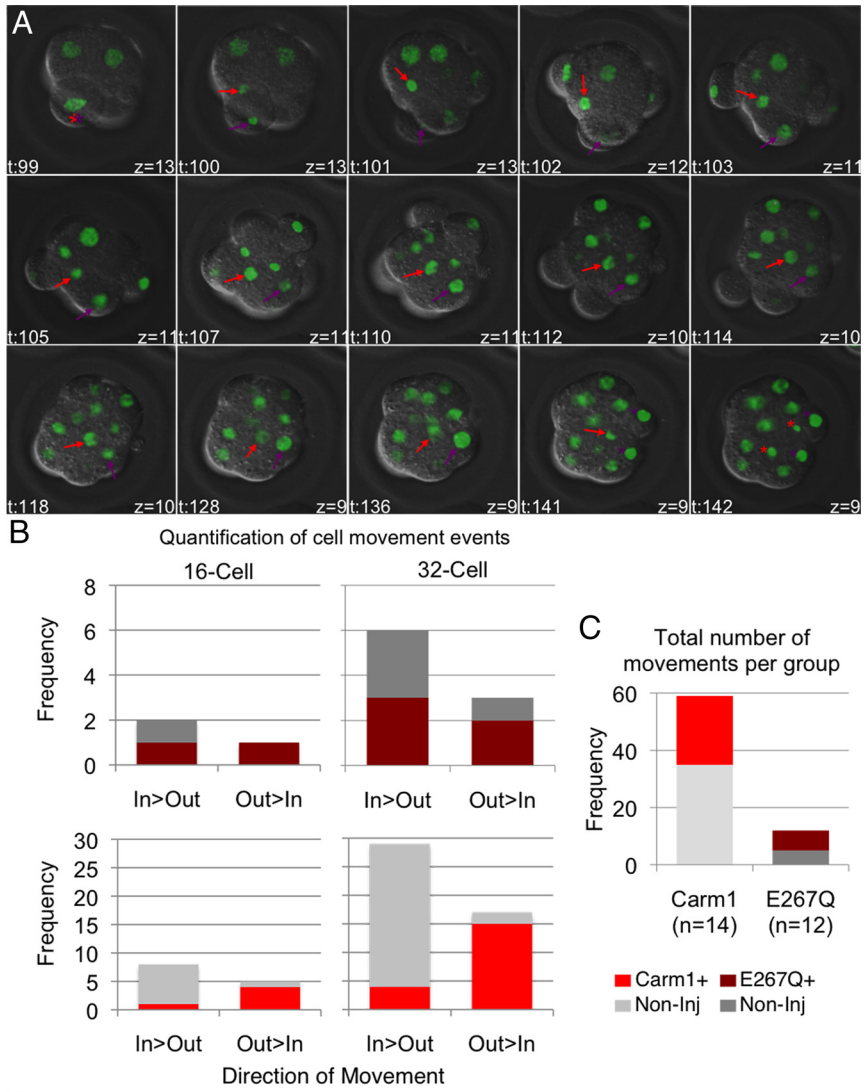

D

p<0.001
p<0.05
p>0.05

		Movement Freq. (%, n)	16-cell movements (%)		32-cell movements (%)	
			IN>OUT	OUT>IN	IN>OUT	OUT>IN
Carm1	Non-Inj	35 (10.4, 336)	7 (88)	1 (12)	25 (93)	2 (7)
(14 embryos)	+	24 (7.14, 336)	1 (20)	4 (80)	4 (21)	15 (79)
Carm1(E267Q)	Non-Inj	6 (2.0, 288)	1 (100)	0 (0)	3 (75)	1 (25)
(12 embryos)	+	7 (2.4, 288)	1 (50)	1 (50)	3 (60)	2 (40)

Figure 2. Carm1 leads to changes in the frequency and direction of cell movement. two-cell blastomeres of H2B-EGFP embryos were injected with *Carm1* (Carm1+) or *Carm1(E267Q)* (E267Q+) and *DsRed* mRNAs, and their development was tracked as in Figure 1. (A) Example illustrating one 16-cell blastomere (red and purple asterisks) dividing symmetrically (time-point 100) producing one daughter (red arrow) moving from an outer to inner position, before dividing again (time-point 142). Z-value indicates plane of view (n = 15), illustrating that the moving cell begins at the top of the embryo, coming to occupy a deeper position within the embryo in this plane as well as in the X-Y plane. (B) Number and direction of movements of noninjected (NonInj) and injected (+) 16- and 32-cell-stage clones under experimental (*Carm1+DsRed*) and control (*Carm1(E267Q)+DsRed*) conditions. (C) Total number of cell movements in groups of embryos injected with *Carm1+dsRed* or *Carm1(E267Q)+DsRed* mRNAs at the two-cell stage. (D) Table summarizing data in B and C. Clones are indicated as positive (+) or negative (NonInj) for *Carm1* or *Carm1(E267Q)* for overexpression. Parentheses indicate cumulative numbers of 16- and 32-cell blastomeres (n) and % of these that alter their position. Legend indicates outcomes of χ^2 tests performed on data outlined in corresponding colors.

ment was observed in 2.3% of all cells (Figure 2, B and D; n = 576 when all 16- and 32-cell blastomeres are considered together). Twenty-five percent (3/12) of these movements occurred during the 16-cell stage, two of which were from an inside to an outside position: one from a noninjected and the other a *Carm1(E267Q)*-injected clone. Of the movements occurring at the 32-cell stage, six of nine were from an inner to an outer position, the noninjected and injected clones making up similar proportions of these movements. Hence, cell movement defined in these terms occurs as often as in unmanipulated embryos and in similar "directions" (Bischoff *et al.*, 2008). In contrast, the frequency of cell movement significantly increased in embryos in which *Carm1* was up-regulated, when compared with both *Carm1(E267Q)*-injected and unmanipulated embryos: 8.7% of all cells were observed to move in *Carm1*-injected embryos (n = 672; 16- and 32-cell blastomeres; Figure 2, C and D) and most of these cell movements (77%, n = 59) occurred during the 32-cell stage. Strikingly, we found that cells with elevated levels of Carm1 tended to move in the opposite direction to their noninjected counterparts in the same embryos (i.e., from an outer to inner position; Figure 2, B and D). Moreover, the frequency of cell movement in the noninjected clone indicated that cells of the noninjected clones moving in the opposite direction might compensate for the behavior of cells of the *Carm1*-injected clone. In agreement with this,

no extra cells were found in the ICM of *Carm1* embryos compared with *Carm1(E267Q)* embryos ($p = 0.69$; Figure 1, A and B). Together with the analysis of division orientation, these results provide evidence that elevation of Carm1 leads cells to adopt ICM positions through both increased frequency of asymmetric divisions and cell movement.

Carm1 Elevation Affects the Expression and Distribution of Par3 and EMK1 in a Reciprocal Manner

To gain further insight into the underlying reasons for our observations on cell dynamics, we examined whether the expression levels and/or distribution of polarity molecules known to govern cell position might be affected by Carm1 up-regulation. We first focused on the cell polarity marker Par3. To compare the expression levels of *Par3* between cells in which Carm1 was up-regulated and those in which it was not in the same embryos, we performed qRT-PCR in three biological samples of cDNA derived from 100 *Carm1*-injected and 100 noninjected blastomeres of 25 disaggregated eight-cell embryos. In control experiments, *Carm1(E267Q)* mRNA replaced that of *Carm1*, as above. To determine whether the disaggregation of blastomeres might have any effect on *Par3* transcript levels, we measured those of whole and disaggregated (but otherwise unmanipulated) eight-cell embryos at the same developmental time point. Low levels of *Par3* transcript were found in all eight-cell cDNA samples (Figure 3A). There was no significant difference between *Par3* levels detected in cDNA derived from whole and disaggregated eight-cell embryos (Figure 3A, Student's *t* test, $p = 0.35$). Similarly, there was no significant difference in these transcript levels between *Carm1*(*E267Q*)-injected cells and their noninjected counterparts (Student's *t* test, $p = 0.62$). In contrast, the levels of *Par3* were 85% lower in the *Carm1*-injected eight-cell clone than in its noninjected counterpart, and, indeed, both control samples (two-way ANOVA; $p < 0.001$, Figure 3A). To determine the extent to which this could also be seen at the protein level, we examined the distribution of Par3 by immunofluorescence. An apical distribution of Par3 was detected in mid-eight-cell blastomeres (Figure 3B), in agreement with one previous report (Plusa *et al.*, 2005) but in contrast to another (Vinot *et al.*, 2005). Furthermore, in agreement with the results of the qRT-PCR experiments, these apical domains of Par3 appeared attenuated in most (90%, 54/60) *Carm1*-injected blastomeres (Figure 3, B and C). In agreement with this, when we quantified the intensity of Par3 domains using Image J, they were on average significantly less in the *Carm1*-injected blastomeres compared with their noninjected counterparts in the same embryos ($p < 0.01$; Figure 3D). This was not observed in *Carm1*(*E267Q*)-injected control embryos (Figure 3, E–G).

To determine whether the changes in cell behavior described above could also reflect the organization of the basolateral pole of eight-cell blastomeres, we examined the distribution of the mammalian homologue of Par1, EMK1, which localizes basolaterally at this stage (Vinot *et al.*, 2005) and is implicated in polarity and cell division regulation in epithelial cells (Bohm *et al.*, 1997). To compare the expression levels of *EMK1* between *Carm1*-injected and noninjected clones in the same embryos, we carried out experiments similar to the ones described for Par3. We found that *EMK1* was detectable in all eight-cell and blastocyst cDNA samples (Figure 4A). We could not find any significant differences in *EMK1* expression between *Carm1(E267Q)*-injected and noninjected clones of the same embryos (Student's *t* test, $p = 0.8$). In contrast we found that *EMK1* transcript levels were 55% higher in *Carm1*-injected than in noninjected cells of the same embryos (Figure 4A). Thus, *EMK1* expression was significantly higher when *Carm1* levels were up-regulated than in all other samples analyzed (two-way ANOVA, $p = 0.013$). To determine the extent to which this could also be seen at the protein level, we examined the distribution of EMK1 protein. Although EMK1 was present throughout the cell, it showed a basolateral accumulation in eight-cell blastomeres as described previously (Vinot *et al.*, 2005). In none of the 13 embryos expressing *Carm1*(*E267Q*) were we able to detect any obvious difference in EMK1 distribution between injected ($n = 52$) and ($n = 52$) noninjected clones (Figure 4, E–G). However, the fluorescent signal of EMK1 appeared stronger, particularly at the basolateral region, in the major-

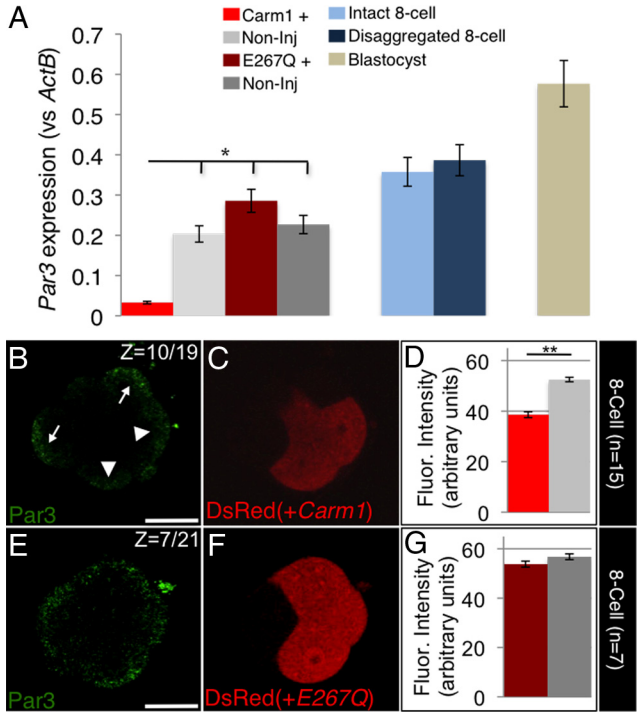

Figure 3. Carm1 leads to decreased *Par3* mRNA expression and protein apicalization. (A) Separated eight-cell blastomeres injected with *Carm1* or *Carm1(E267Q)* and *DsRed* mRNAs at the two-cell stage were pooled into noninjected (NonInj) and injected (+) samples used for qRT-PCR. Normalized averages of biological and technical triplicate are shown. Blastocyst cDNA was used as a positive control. As a disaggregation control, cDNA from 25 intact eight-cell embryos and 25 disaggregated eight-cell embryos was used in the same way. Normalized averages of biological duplicate and technical triplicate are shown for these groups. Error bars, SEM. *Par3* transcripts were lower in *Carm1*-injected clones than in *Carm1(E267Q)*-injected and both noninjected samples (two-way ANOVA, $^*p < 0.001$). (B–G) Embryos treated as in A were fixed at the eight-cell stage and immunostained for Par3. Weaker Par3 domains (arrowheads) were associated with *Carm1* injected clones (54/60 blastomeres, $n = 15$ embryos), than noninjected clones of the same embryos (arrows; B–D). This trend was not observed in the 28 blastomeres of seven control embryos (E–G). Scale bars, 20 μm. Z value indicates plane of view (/n). (D and G) Graphs indicating the mean fluorescence intensity of Par3 domains, measured for each cell in alternate Z-sections using Image J and calculated for the *Carm1*/*Carm1(E267Q)*-injected and noninjected cell populations. Error bars, SEM. Student's *t* test, $^{**}p < 0.01$.

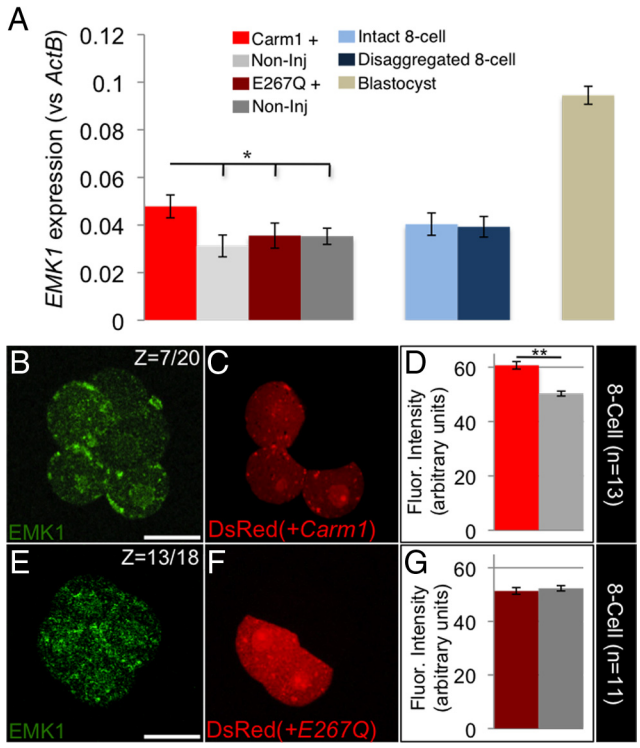

Figure 4. Carm1 leads to increased *EMK1* mRNA levels and changes to EMK1 protein distribution. (A) Separated eight-cell blastomeres injected with *Carm1* or *Carm1(E267Q)* and *DsRed* mRNAs at the two-cell stage were pooled into noninjected (NonInj) and injected (+) samples used for qRT-PCR. Normalized averages of biological and technical triplicate are shown. Blastocyst cDNA was used as a positive control. As a disaggregation control, cDNA from 25 intact eight-cell embryos and 25 disaggregated eight-cell embryos was used in the same way. Normalized averages of biological duplicate and technical triplicate are shown for these groups. Error bars, SEM. *EMK1* transcripts were higher in *Carm1*-injected clones than *Carm1(E267Q)*-injected and both noninjected clones (two-way ANOVA, *p = 0.013). (B–G) Embryos treated as in A were fixed at the eight-cell stage and immunostained for EMK1. Stronger EMK1 basolateral domains (arrows) were associated with *Carm1*-positive clones (36/46 blastomeres, n = 12 embryos) than the control clones in the same embryos (B–D). This trend was not observed in 104 blastomeres analyzed from 13 control embryos (E–G). Scale bars, 20 μm. Z value indicates plane of view (/n). (D and G) Graphs indicating the mean fluorescence intensity of EMK1 domains, measured for each cell in alternate Z-sections using Image J and calculated for the *Carm1*/*Carm1(E267Q)*-injected and noninjected cell populations. Error bars, SEM. Student's *t* test, **p = 0.024.

ity (75%, 36/48) of *Carm1*-injected blastomeres (n = 48) compared with their noninjected neighbors (n = 48; Figure 4, B and C). When we quantified this, we found that the intensity of the EMK1 signal was indeed significantly greater in *Carm1*-injected blastomeres than in their noninjected counterparts in the same embryos (p = 0.024; Figure 4D). Together these results suggest that elevated expression of Carm1 affects the expression and distribution of Par3 and EMK1 in a reciprocal manner, a decrease in Par3 expression and apical distribution being associated with an increase in EMK1 expression and basolateral distribution. Thus, elevation of Carm1 leads to an alteration of the expression and distribution of molecules known to regulate mammalian cell polarity and associate with changes in division asymmetry (Bohm *et al.*, 1997; Plusa *et al.*, 2005).

Carm1 Elevation Increases the Expression of the aPKC Antagonist, PKCII

Because of the role demonstrated for the λ isoform of aPKC in affecting division orientation during mouse development (Plusa *et al.*, 2005) and pole size in *Xenopus* embryos (Chalmers *et al.*, 2005), we wondered whether the increased frequency of asymmetric division and cell internalization associated with Carm1 up-regulation is also associated with changes in the expression or distribution of aPKCζ. To this end, we first characterized the distribution of aPKCζ protein from the two-cell stage to the late morula stage in normal development (Figure 5). Initially, aPKCζ appears to be distributed uniformly at the cell cortex until the eight-cell stage (Figure 5, A and B). However, this changes after compaction, when aPKCζ distribution becomes distinctively apical at the mid-eight-cell stage (Figure 5C) and is more evenly distributed over the apical cell membrane from the late eight-cell stage onward; it also shows a detectable concentration at the outer surface of the developing morula (Figure 5D). We also quantified *aPKCζ* expression in total RNA extracts of intact, unmanipulated embryos through developmental time. This revealed a peak in *aPKCζ* levels concomitant with its change in distribution at the eight-cell stage (Figure 5I).

To compare aPKCζ distribution between cells in which Carm1 was elevated and their noninjected neighbors, mid-eight-cell embryos expressing *Carm1* and *DsRed* mRNAs in the progeny of one two-cell blastomere were fixed and stained with antibody specific to the kinase-containing C-terminus of aPKCζ. This revealed that in 89% (85/96, n = 24 embryos) of blastomeres with higher levels of Carm1, the apical domains of aPKCζ appeared more concentrated than in the noninjected neighboring blastomeres (Figure 5, K–N). Such differences were not apparent between the injected and noninjected clones of *Carm1(E267Q)* embryos (Figure 5, O and P; n = 11 embryos). Indeed, when we quantified the intensities of aPKCζ domains, they were significantly higher in the blastomeres in which Carm1 was elevated than their counterparts with nonelevated Carm1 levels in the same embryos ($p < 0.01$; Figure 5M), a trend we did not observe in *Carm1(E267Q)*-injected control embryos (Figure 3P). To test this further, we analyzed *aPKCζ* transcript levels using eight-cell cDNA samples as above: Levels in cells with elevated Carm1 were 56% higher than in the noninjected cells of the same embryos, a difference not seen between injected and noninjected cells in *Carm1(E267Q)* embryos (Figure 5Q; two-way ANOVA, p = 0.0005).

In some respects, this was an unexpected result, as the effect on Par3/EMK1 expression and distribution suggested a "depolarizing" phenotype for Carm1 up-regulation. Moreover, down-regulation of aPKCλ promotes asymmetric division and cell internalization (Plusa *et al.*, 2005), similar to the effects described here for up-regulation of Carm1. However, although overexpression of aPKCλ is sufficient to induce cell protrusion in *Xenopus* embryos, overexpression of a truncated version of the protein, lacking the kinase domain, does not produce this phenotype (Chalmers *et al.*, 2005). This drew our attention to a previously reported isoform, PKCII, showing 98% amino acid identity with aPKCζ but lacking the kinase domain (Parkinson *et al.*, 2004). Because the interaction domains of these proteins are functionally identical, PKCII is proposed to regulate the activity of aPKCζ by competing for sites of activity in mammalian epithelial cell culture (Parkinson *et al.*, 2004). To date, there have been no reports of whether a similar mechanism might occur in the mouse embryo, so we wanted to examine whether *PKCII* expression could be positively affected by

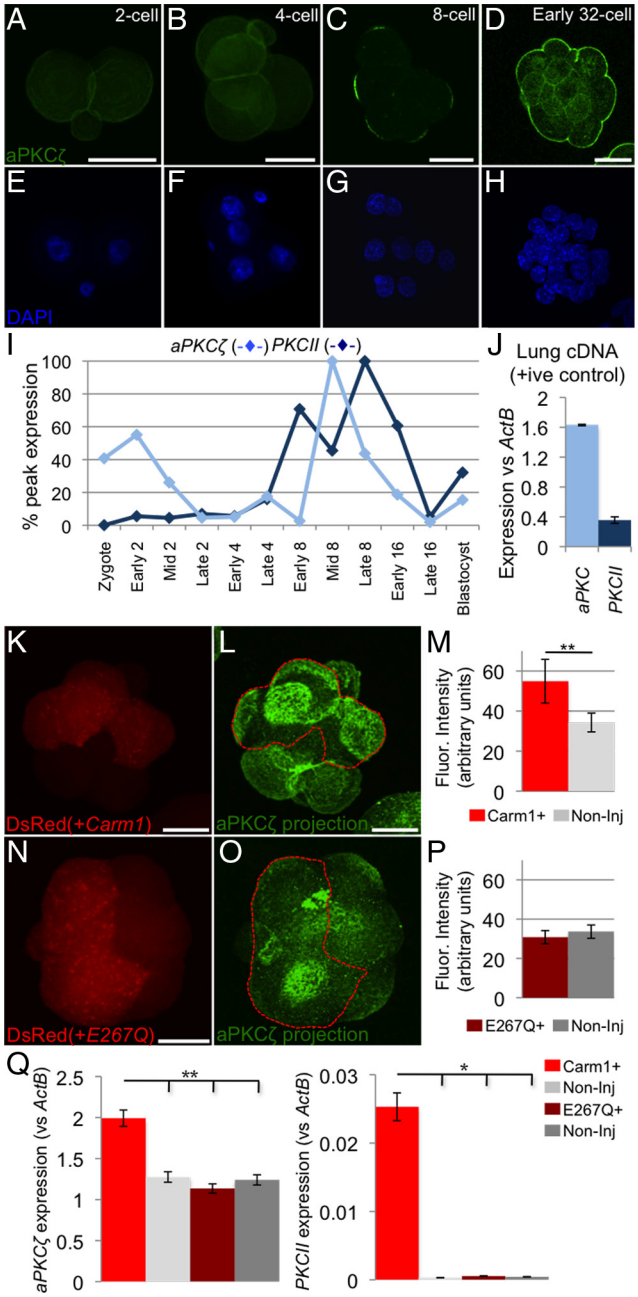

Figure 5. Carm1 leads to increased expression of the *aPKCζ* antagonist, *PKCII*. (A–H) aPKCζ protein in two-cell (n = 5), 4-cell (n = 7), mid-eight-cell (n = 28), and early 32-cell (n = 8) embryos. (I) *aPKCζ* and *PKCII* expression measured at several time points, plotted as % of peak expression. (J) Normalized levels of *aPKCζ* and *PKCII* transcripts measured by qRT-PCR using lung cDNA. Averages of biological duplicate and technical triplicate are shown. Error bars, SEM. (K–P) Embryos treated as in A were examined for aPKCζ at the eight-cell stage. Examples illustrate stronger apical aPKCζ domains associated with *Carm1*-injected clones (outlined in red; 85/96 blastomeres, n = 24 embryos) than the noninjected clones in the same embryos (K–L). This trend was not observed in the 84 blastomeres from 11 control embryos (N and O). Scale bars, 20 μm. (M, P) Graphs indicating the mean fluorescence intensity of aPKCζ domains, measured for each cell in alternate Z-sections using Image J and calculated for the *Carm1*/*Carm1(E267Q)*-injected and noninjected cell populations. Error bars, SEM. Student's *t* test, **p < 0.01. (Q) Separated eight-cell blastomeres injected with *Carm1* or *Carm1(E267Q)* and *DsRed* mRNAs at the two-cell stage were pooled into noninjected (NonInj) and injected (+) samples used for qRT-PCR. Normalized averages of biological and technical triplicate are shown. Error bars, SEM. *aPKCζ* and *PKCII* transcripts were higher in *Carm1*-injected clones than *Carm1(E267Q)*-injected and both noninjected clones. Two-way ANOVA, *p = 0.0005, **p = 0.003.

Carm1 overexpression. Using primers specific for this particular isoform and lung cDNA as a positive control, we found that expression of *PKCII* is indeed detectable in the mouse embryo, although at lower levels than *aPKCζ* (Figure 5, I and J). This finding led us to analyze changes in *PKCII* expression levels throughout preimplantation development, which revealed a peak in its expression at the late eight-cell stage (Figure 5I). To determine whether a change in *PKCII* expression could be associated with Carm1 up-regulation, we next compared the level of *PKCII* transcript in eight-cell stage cells with higher levels of Carm1 with that of noninjected clones in the same embryos. This revealed that *PKCII* levels were 77-fold higher in cells in which Carm1 was elevated (Figure 5Q). Such a difference was not seen between injected and noninjected blastomeres in *Carm1(E267Q)* embryos. Thus *PKCII* levels in *Carm1*-injected cells were significantly higher than in all other samples ($p = 0.0032$; Figure 6K). This striking increase in *PKCII* expression observed upon Carm1 up-regulation could affect normal aPKCζ function at the apical pole.

Carm1 Elevation Leads to Decreased Expression of Cdx2

The transcription factor Cdx2 is key for TE formation (Niwa *et al.*, 2005; Strumpf *et al.*, 2005; Jedrusik *et al.*, 2008; Nishioka *et al.*, 2009) and its down-regulation increases the probability with which cells take asymmetric rather than symmetric division (Jedrusik *et al.*, 2008). We therefore wondered whether Carm1 up-regulation affects the level of Cdx2 expression. To address this, we measured *Cdx2* transcript levels in cells in which Carm1 was up-regulated and compared them with those of noninjected cells of the same embryos, as above. This revealed that the expression of *Cdx2* was 70% lower in cells with higher levels of Carm1 (Figure 6A). This was in contrast to the levels of *Cdx2* observed between injected and noninjected blastomeres in *Carm1(E267Q)* embryos, which were statistically comparable. Thus, Carm1 overexpression results in a significant reduction in *Cdx2* expression (two-way ANOVA, $p < 0.001$).

Because Cdx2 expression shows heterogeneity at the eight-cell stage, we extended the above analysis and examined the proportions of Cdx2-positive nuclei in blastomeres with different levels of Carm1 at the eight-cell stage (Figure 6, B and C). From 19 embryos in which Carm1 was overexpressed, 60 eight-cell blastomeres were Cdx2-positive (Figure 6D). Of these, only 22 were derived from these cells in which *Carm1* was injected ($\chi^2 = 4.28$, $p = 0.039$). Taken together, these results provide evidence that Cdx2 is expressed to a lesser extent upon Carm1 up-regulation, but also indicate that this association can be affected by the endogenous variability in Cdx2, previously observed among eight-cell blastomeres (Ralston and Rossant, 2008; Jedrusik *et al.*, 2008). This may parallel the natural heterogeneity in Carm1-modified histone substrates observed at this time (Torres-Padilla *et al.*, 2007).

DISCUSSION

The divisions that internalize cells contribute to the first differentiation event that separates ICM from TE in the mouse embryo. Carm1 could play an important role in this

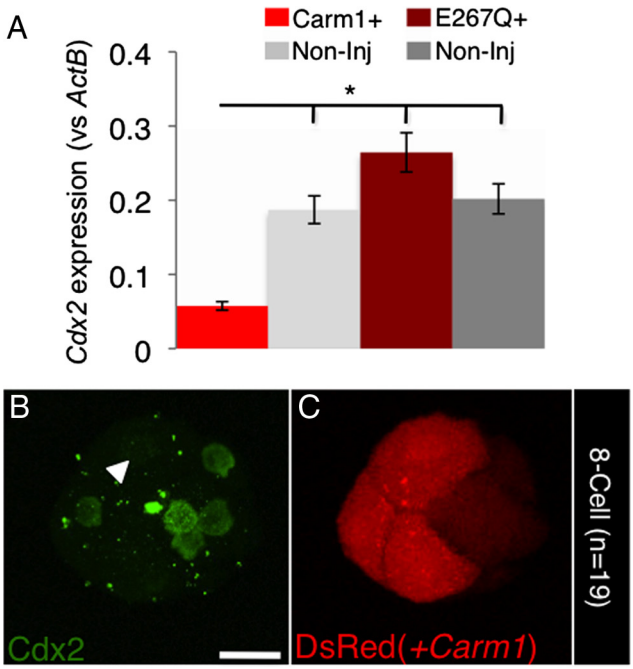

D

	Carm1+	Non-Inj
Observed	22*	38*
Expected	30.00	30.00

*p=0.039, X^2 test

Figure 6. Carm1 leads to a down-regulation of Cdx2. (A) Separated eight-cell blastomeres injected with *Carm1* or *Carm1(E267Q)* and *DsRed* mRNAs at the two-cell stage were pooled into noninjected (NonInj) and injected (+) samples used for qRT-PCR. Normalized averages of biological and technical triplicate are shown. Error bars, SEM. *Cdx2* transcripts were lower in *Carm1*-injected clones than *Carm1(E267Q)*-injected and both noninjected clones. Two-way ANOVA; *$p < 0.001$. (B and C) Eight-cell embryos treated as in A were fixed and immunostained for Cdx2. Six blastomeres in the example are Cdx2-positive, one weakly so (arrowhead). Of these, four derive from the noninjected clone. Scale bar, 20 μm. (D) Frequencies of Cdx2-positive nuclei in *Carm1* overexpressing (Carm1+) and noninjected blastomeres (NonInj) from 19 embryos.

process, as its up-regulation was shown to lead to a higher proportion of cells becoming ICM (Torres-Padilla *et al.*, 2007). The mechanism by which this is achieved and whether differences in Carm1 levels could culminate in altered expression of genes that direct cell division, and hence cell allocation and lineage determination, have remained unknown. Our study provides evidence that Carm1 expression influences cell polarity and the expression of genes that affect the allocation of cells to the ICM versus TE lineages. We find that higher levels of Carm1 lead to more asymmetric divisions and cell internalization in association with reduced expression and diminished localization of Par3 apically and increased expression of the basolateral marker EMK1. Finally, our results suggest an involvement of the aPKC antagonist, PKCII, and Cdx2 in this process.

The analysis of behavior and gene expression of cells with differing levels of Carm1 developing side-by-side gives insight into how endogenous heterogeneity in Carm1, and differential modification of its targets such as H3R26/R17 (Torres-Padilla *et al.*, 2007), contribute to the mechanisms of inner cell allocation during preimplantation development. Levels of Carm1 have been reported to vary in four-cell blastomeres, showing the same tendencies as those of H3R26me2 (Torres-Padilla *et al.*, 2007), raising the possibility that endogenous heterogeneity of this enzyme has an impact on development, particularly in directing cells to the different blastocyst lineages. The consequences of experimentally elevating Carm1, we now report, add to these findings and indicate that differences in Carm1 levels among cells could influence cell dynamics. It will be of future interest to study the effects of Carm1 elimination at these early stages. To date this has only been achieved in zygotes injected with AMI-1, an inhibitor of arginine methyltransferase activity that preferentially targets Carm1 in vitro (Cheng *et al.*, 2004). Such injection led to developmental arrest after just one mitotic division (Torres-Padilla *et al.*, 2007). This experiment most likely targeted maternally supplied Carm1, since loss of zygotic Carm1 expression in *Carm1*$^{-/-}$ embryos permitted survival to perinatal stages (Yadav *et al.*, 2003).

Blastomeres with higher levels of Carm1 up-regulate pluripotency genes such as Nanog and Sox2 (Torres-Padilla *et al.*, 2007). This is likely to prime cells to become ICM, whereas the changes in expression of cell polarity genes that we report here would facilitate asymmetric division and cell movement to fulfil this acquired potential. This suggests that an inherent or induced molecular signature can override signals from, or lead to an alteration in, cell position. In keeping with the first of these possibilities, inner cells have been demonstrated to retain inner identity while still having a portion of their surface exposed to the perivitiline space (PVS; Pederson *et al.*, 1986). Thus, assessment of the proportion of a cells' surface exposed to the PVS may not always accurately identify cells as inner or outer. Moreover, the cell movement we observe here demonstrates that cell fate is not yet fixed at this stage, in agreement with earlier reports (Rossant and Vijh, 1980; Fleming, 1987; Suwinska *et al.*, 2008). The tracking of cells with differing levels of Carm1 side-by-side in the same embryos suggests that such cell sorting may stem from conflicting influences between external (positional) cues and the more inherent molecular signature of a cell. The inward movement of cells with higher Carm1 levels and outward movement of their neighbors are thus representative of cells' plasticity with regard to adopting new positions within the embryo, depending on their induced/inherent molecular signature. The observation that cells in which Carm1 was not elevated tend to move outward might illustrate compensation for inward movement of cells with high Carm1 levels, so that the total number of inside and outside remains similar, emphasizing the plasticity of the embryo. Supportive of this idea are the results of experiments in which Carm1 was overexpressed in the zygote. Time-lapse analysis reveals that the average proportion of asymmetric divisions taken during the 8–16-cell transition in these embryos is greater than that of nonmanipulated embryos at the same stage ($p < 0.001$, Supplemental Figure 2A). A similar, though weaker, trend is seen at the 16–32-cell stage ($p = 0.041$, Supplemental Figure 2A). Interestingly, this is reflected in the average proportion of inner cells per blastocyst analyzed—greater in embryos injected with *Carm1* at the zygote stage than in those injected at the two-cell stage with *Carm1* or *Carm1(E267Q)* (Supplemental Figure 2, B and C). Together this adds weight to the observed effect of increasing Carm1 levels on cell dynamics, which also further suggest that reciprocal movement of unmanipulated cells only compensate for changes in cell division pattern in particular contexts. Thus, intercellular variation in the levels

(and activity) of Carm1 could be as influential as its presence or absence. It is likely that when blastomeres with higher levels of Carm1 develop alongside those in which Carm1 levels are lower, a sorting mechanism could relieve potential conflicts between positional signals and cell identity resulting from, for example, the up-regulation of Nanog and Sox2 (Torres-Padilla *et al.,* 2007). Such a mechanism could be applicable to normal development in so far as endogenous variation in the expression and/or activity of Carm1 (Torres-Padilla *et al.,* 2007) could account for patterns of cell behavior (Fujimori *et al.,* 2003; Piotrowska-Nitshe *et al.,* 2005; Bischoff *et al.,* 2008).

The expression of several molecules regulating cell polarity is changed upon up-regulation of Carm1. *Par3* transcripts are reduced by 84% at the eight-cell stage in *Carm1*-overexpressing clones and the apical distribution of its protein is weaker than in noninjected blastomeres of the same embryos, although not completely lost. The consequences for this reduction could relate to the role of Par3 as a scaffold protein: Its interaction with Par6 and aPKC is key to the control of polarity and spindle orientation in different animal cells and manipulation of its expression is sufficient to disrupt regulation of polarity and cell division (Hirose *et al.,* 2002). Conversely, its down-regulation in individual blastomeres leads their progeny to contribute more cells to the ICM (Plusa *et al.,* 2005). Though it is clear, therefore, that Par3 is involved in the onset of cell polarity, it is not clear whether (or if so, how) Par3 regulates cell division. The correlative evidence we present here would suggest this to be possible, whether indirectly or otherwise, at the 8–16-cell transition. The binding and activation of CDC42, a Rho-family GTPase (Mackay and Hall, 1998) by Par3 could represent a mechanism through which this might take place, potentially accounting for the effects on cell division and movement we see in parallel to changes in Par3 distribution. Because Par3 protein was still detected apically to some extent in cells with higher levels of Carm1, molecules making a basal contribution to cell polarity might also respond to Carm1 and contribute to the phenotype we observe here.

In agreement with this, we find that Carm1 up-regulation leads to a change in the expression and localization of EMK1, which is localized basolaterally in eight-cell blastomeres (Vinot *et al.,* 2005 and this article). This change could accord with a role for this molecule in positioning the spindle and influencing cell–cell contacts, as observed in other cell types (Bohm *et al.,* 1997). Such functions might be mediated through its interaction with microtubule-associated proteins (MAPs); the rat homologue, MARK-2, phosphorylates several MAPs in vivo and by so doing detaches them from microtubules (Drewes *et al.,* 1997). An increase in EMK1 could therefore be partly responsible for the effects of Carm1 up-regulation; it could destabilize microtubule dynamics and, combined with attenuation of Par3 at the apical pole, randomize the axes of cell division at the eight-cell stage, making divisions less likely to conform to structurally imposed tendencies. The "inside" properties conferred by high levels of Carm1 could then "push" cells to move inward. Differences in cell adhesion, resulting from expression of molecules such as E-cadherin (E-cad), could be involved in such a scenario. This protein becomes enriched at regions of cell–cell contact during compaction (Vestweber *et al.,* 1987), and although *E-cad*$^{-/-}$ embryos undergo compaction at the eight-cell stage, the increased cell–cell contacts are not maintained and embryos do not develop to normal blastocysts (Riethmacher *et al.,* 1995). However, our studies do not reveal any significant change in *E-cad* expression in response to the overexpression of Carm1, either at the eight- or16-cell stage (Supplemental Figure 3). Indeed, other mechanisms could also feature in this process, such as the cytoskeletal and shape changes recently suggested (Dard *et al.,* 2009).

The observed strengthening of apical aPKCζ domains at the mid-eight-cell stage along with increased *aPKCζ* mRNA levels upon Carm1 up-regulation was unexpected. Overexpression of aPKCλ in *Xenopus* embryos results in an expansion of blastomere apical domains (Chalmers *et al.,* 2005). In agreement with this, down-regulation of aPKCλ is associated with cell internalization (Plusa *et al.,* 2005; Dard *et al.,* 2009), particularly when individual cells are targeted (Dard *et al.,* 2009). The similarity of this phenotype with that of Carm1 overexpression makes the changes in aPKCζ expression and distribution we observe puzzling. However, it is unclear whether the strengthening of aPKCζ domains and increased mRNA levels are sufficient to bring about phenotypic alteration, especially because the changes in aPKCζ distribution we observe are less dramatic than those associated with up-regulation of Cdx2 (Jedrusik *et al.,* 2008). Indeed, aPKCλ up-regulation appears to have no impact on cell allocation and embryo development in the mouse, despite the impact of its depletion in the same context (Dard *et al.,* 2009). However, there are important differences in the normal distribution and function of these isoforms (Thomas *et al.,* 2004; Dard *et al.,* 2009), which show 71% amino acid sequence identity (Parkinson *et al.,* 2004). Thus, changes in aPKCζ could have consequences different from those of aPKCλ. Bearing this in mind, our finding of a 77-fold increase in the aPKCζ antagonist, *PKCII,* transcript levels upon Carm1 elevation seem likely to be important in the interpretation of our results. PKCII would compete with endogenous aPKCζ for its binding sites. Furthermore, the time course of *aPKCζ* and *PKCII* expression in embryos suggest an endogenous mechanism for the regulation of aPKCζ function. At least one target of aPKCζ is Par3: the binding and phosphorylation of Par3 by aPKC, along with the association of Par6, is crucial to its function (Lin *et al.,* 2000; Hirose *et al.,* 2002). Because the Par3 message and protein appears to be reduced upon Carm1 elevation, any changes in aPKCζ distribution may have less relevance. A similar conclusion may be drawn from the finding that basolateral EMK1 domains are strengthened in blastomeres with higher levels of Carm1. Taken together, it seems unlikely that Carm1 could be exerting its effects on division orientation and polarity through aPKCζ alone.

It is also interesting to consider the relationship between aPKCζ expression and Cdx2. Although *Cdx2* mRNA is present at low levels as early as the four-cell stage (Wang *et al.,* 2004; Jedrusik *et al.,* 2008), nuclear Cdx2 protein appears at the eight-cell stage and seems to be downstream of blastomere polarization (Ralston and Rossant, 2008). However, upon overexpression, Cdx2 is able to induce cell polarization, as evidenced by stronger aPKCζ domains (Jedrusik *et al.,* 2008). Here, we report that up-regulation of Carm1 leads to a reduction in Cdx2 expression, on mRNA and protein levels, at the eight-cell stage. Although this is in accord with the effect of Carm1 up-regulation on cell fate and Nanog and Sox2 expression (Torres-Padilla *et al.,* 2007), it seems unlikely to be a direct response, because the promoter of Cdx2 is not enriched for Carm1 binding or H3R26/17 methylation, at least in ES cells (Wu *et al.,* 2009). Thus, it is tempting to speculate a role for increased PKCII expression in the down-regulation of aPKCζ, and hence *Cdx2* mRNA and protein, expression we observe here, in keeping with an inner, as opposed to outer, cell identity. Indeed, expression of Cdx2 in the inner cells is lost by the blastocyst stage (Dietrich and Hiiragi, 2007; Ralston and Rossant, 2008; Jedrusik *et al.,* 2008)

and is essential to the specification and maintenance of TE cell fate (Strumpf *et al.*, 2005).

Although it is quite likely that the effect of Carm1 in up-regulating pluripotency and down-regulating apical polarity of cells reflects its role in histone methylation and transcriptional coactivation of nuclear receptors (Chen *et al.*, 1999), Carm1 also regulates many other processes (Wysocka, 2006; Kowenz-Leutz *et al.*, 2010). As well as R17 and 26 on histone H3, Carm1 targets H3 R128, 129, 131, and 134 and H2A for methylation, in turn associated with up-regulation of gene expression (Zhang and Reinberg, 2001). These modifications are generally considered as long-term epigenetic marks, essential to the activation of specific gene expression patterns (Lachner *et al.*, 2004). However, Carm1 can also cooperate with transcription factors such as p53 (An *et al.*, 2004) and p300 (Chen *et al.*, 2000) and change chromatin structure at particular promoters—putatively of genes such as Nanog and Sox2 (Torres-Padilla *et al.*, 2007)—and thereby sustain pluripotency. This would prime cells with inner cell properties, facilitating processes mediated by Par3 and EMK1. Notwithstanding these possibilities, the results presented here bring us closer to linking an epigenetic mark to the derivation of the ICM, most likely through the effect of Par3 and EMK1 upon cell polarity, division mechanics and movements.

ACKNOWLEDGMENTS

We are grateful to M.Z.-G. lab members for support and discussions and to Kat Hadjantonakis (Sloan-Kettering, New York, NY) and Ginny Papaioannou (Columbia University, New York, NY) for the reporter transgenic line. This work was supported by the Wellcome Trust Senior Research Fellowship to M.Z.-G. and MCR Studentship to D.-E.P.

REFERENCES

An, W., Kim, J., and Roeder, R. G. (2004). Ordered cooperative functions of PRMT1, p300, and CARM1 in transcriptional activation by p53. Cell *117*, 735–748.

Barlow, P., Owen, D. A., and Graham, C. (1972). DNA synthesis in the preimplantation mouse embryo. J. Embryol. Exp. Morphol. *27*, 431–445.

Bischoff, M., Parfitt, D.-E., and Zernicka-Goetz, M. (2008). Formation of the embryonic-abembryonic axis of the mouse blastocyst: relationships between orientation of early cleavage divisions and pattern of symmetric/asymmetric divisions. Development *135*, 953–962.

Bohm, H., Brinkmann, V., Drab, M., Henske, A., and Kurzchalia, T. V. (1997). Mammalian homologues of *C. elegans* PAR-1 are asymmetrically localized in epithelial cells and may influence their polarity. Curr. Biol. *7*, 603–606.

Chalmers, A. D., Pambos, M., Mason, J., Lang, S., Wylie, C., and Papalopulu, N. (2005). aPKC, Crumbs3 and Lgl2 control apicobasal polarity in early vertebrate development. Development *132*, 977–986.

Chen, D., Huang, S. M., and Stallcup, M. R. (2000). Synergistic, p160 coactivator-dependent enhancement of estrogen receptor function by CARM1 and p300. J. Biol. Chem. *275*, 40810–40816.

Chen, D., Ma, H., Hong, H., Koh, S. S., Huang, S. M., Schurter, B. T., Aswad, D. W., and Stallcup, M. R. (1999). Regulation of transcription by a protein methyltransferase. Science *284*, 2174–2177.

Cheng, D., Yadav, N., King, R. W., Swanson, M. S., Weinstein, E. J., and Bedford, M. T. (2004). Small molecule regulators of protein arginine methyltransferases. J. Biol. Chem. *279*, 23892–23899.

Dard, N., Le, T., Maro, B., and Louvet-Vallée, S. (2009). Inactivation of aPKClambda reveals a context dependent allocation of cell lineages in preimplantation mouse embryos. PLoS One *4*, e7117.

Dietrich, J. E., and Hiiragi, T. (2007). Stochastic patterning in the mouse pre-implantation embryo. Development *134*, 4219–4231.

Drewes, G., Ebneth, A., Preuss, U., Mandelkow, E. M., and Mandelkow, E. (1997). MARK, a novel family of protein kinases that phosphorylate microtubule-associated proteins and trigger microtubule disruption. Cell *89*, 297–308.

Dyce, J., George, M., Goodall, H., and Fleming, T. P. (1987). Do trophectoderm and inner cell mass cells in the mouse blastocyst maintain discrete lineages? Development *100*, 685–698.

Erhardt, S., Lyko, F., Ainscough, J. F., Surani, M. A., and Paro, R. (2003). Polycomb-group proteins are involved in silencing processes caused by a transgenic element from the murine imprinted H19/Igf2 region in Drosophila. Dev. Genes Evol. *213*, 336–344.

Fleming, T. P. (1987). A quantitative analysis of cell allocation to trophectoderm and inner cell mass in the mouse blastocyst. Dev. Biol. *119*, 520–531.

Goldstein, B., and Macara, I. G. (2007). The PAR proteins: fundamental players in animal cell polarization. Dev. Cell *13*, 609–622.

Hadjantonakis, A. K., and Papaioannou, V. E. (2004). Dynamic in vivo imaging and cell tracking using a histone fluorescent protein fusion in mice. BMC Biotechnol. *4*, 33.

Hirose, T., *et al.* (2002). Involvement of ASIP/PAR-3 in the promotion of epithelial tight junction formation. J. Cell Sci. *115*, 2485–2495.

Houliston, E., Pickering, S. J., and Maro, B. (1989). Alternative routes for the establishment of surface polarity during compaction of the mouse embryo. Dev. Biol. *134*, 342–350.

Hurov, J. B., Watkins, J. L., and Piwnica-Worms, H. (2004). Atypical PKC phosphorylates par-1 kinases to regulate localization and activity. Curr. Biol. *14*, 736–741.

Jedrusik, A., Parfitt, D. E., Guo, G., Skamagki, M., Grabarek, J. B., Johnson, M. H., Robson, P., and Zernicka-Goetz, M. (2008). Role of Cdx2 and cell polarity in cell allocation and specification of trophectoderm and inner cell mass in the mouse embryo. Genes Dev. *22*, 2692–2706.

Johnson, M. H., and Ziomek, C. A. (1981a). Induction of polarity in mouse 8-cell blastomeres: specificity, geometry, and stability. J. Cell Biol. *91*, 303–308.

Johnson, M. H., and Ziomek, C. A. (1981b). The foundation of two distinct cell lineages within the mouse morula. Cell *24*, 71–80.

Kowenz-Leutz, E., Pless, O., Dittmar, G., Knoblich, M., and Leutz, A. (2010). Crosstalk between C/EBPbeta phosphorylation, arginine methylation, and SWI/SNF/Mediator implies an indexing transcription factor code. EMBO J. *29*, 1105–1115.

Lachner, M., Sengupta, R., Schotta, G., and Jenuwein, T. (2004). Trilogies of histone lysine methylation as epigenetic landmarks of the eukaryotic genome. Cold Spring Harb. Symp. Quant. Biol. *69*, 209–218.

Lee, Y. H., Koh, S. S., Zhang, X., Cheng, X., and Stallcup, M. R. (2002). Synergy among nuclear receptor coactivators: selective requirement for protein methyltransferase and acetyltransferase activities. Mol. Cell Biol. *22*, 3621–3632.

Lin, D., Edwards, A. S., Fawcett, J. P., Mbamalu, G., Scott, J. D., and Pawson, T. (2000). A mammalian PAR-3-PAR-6 complex implicated in Cdc42/Rac1 and aPKC signalling and cell polarity. Nat. Cell Biol. *2*, 540–547.

Mackay, D. J., and Hall, A. (1998). Rho GTPases. J. Biol. Chem. *273*, 20685–20688.

Nakaya, M., Fukui, A., Izumi, Y., Akimoto, K., Asashima, M., and Ohno, S. (2000). Meiotic maturation induces animal-vegetal asymmetric distribution of aPKC and ASIP/PAR-3 in *Xenopus* oocytes. Development *127*, 5021–5031.

Nishioka, N., *et al.* (2009). The Hippo signaling pathway components Lats and Yap pattern Tead4 activity to distinguish mouse trophectoderm from inner cell mass. Dev. Cell *16*, 398–410.

Niwa, H., Toyooka, Y., Shimosato, D., Strumpf, D., Takahashi, K., Yagi, R., and Rossant, J. (2005). Interaction between Oct3/4 and Cdx2 determines trophectoderm differentiation. Cell *123*, 917–929.

O'Neill, L. P., VerMilvea, M. D., and Turner, B. M. (2006). Epigenetic characterization of the early embryo with a chromatin immunoprecipitation protocol applicable to small cell populations. Nat. Genet. *38*, 835–841.

Parkinson, S. J., Le Good, J. A., Whelan, R. D., Whitehead, P., and Parker, P. J. (2004). Identification of PKCzetaII: an endogenous inhibitor of cell polarity. EMBO J. *23*, 77–88.

Pedersen, R. A., Wu, K., and Bałakier, H. (1986). Origin of the inner cell mass in mouse embryos: cell lineage analysis by microinjection. Dev. Biol. *117*, 581–595.

Piotrowska-Nitsche, K., Perea-Gomez, A., Haraguchi, S., and Zernicka-Goetz, M. (2005). Four-cell stage mouse blastomeres have different developmental properties. Development *132*, 479–490.

Plusa, B., Frankenberg, S., Chalmers, A., Hadjantonakis, A. K., Moore, C. A., Papalopulu, N., Papaioannou, V. E., Glover, D. M., and Zernicka-Goetz, M. (2005). Downregulation of Par3 and aPKC function directs cells towards the ICM in the preimplantation mouse embryo. J. Cell Sci. *118*, 505–515.

Ralston, A., and Rossant, J. (2008). Cdx2 acts downstream of cell polarization to cell-autonomously promote trophectoderm fate in the early mouse embryo. Dev. Biol. *313*, 614–629.

Riethmacher, D., Brinkmann, V., and Birchmeier, C. (1995). A targeted mutation in the mouse E-cadherin gene results in defective preimplantation development. Proc. Natl. Acad. Sci. USA *92*, 855–859.

Rossant, J., and Vijh, K. M. (1980). Ability of outside cells from preimplantation mouse embryos to form inner cell mass derivatives. Dev. Biol. *76*, 475–482.

Schnabel, R., Hutter, H., Moerman, D., and Schnabel, H. (1997). Assessing normal embryogenesis in *Caenorhabditis elegans* using a 4D microscope: variability of development and regional specification. Dev. Biol. *184*, 234–265.

Schurter, B. T., Koh, S. S., Chen, D., Bunick, G. J., Harp, J. M., Hanson, B. L., Henschen-Edman, A., Mackay, D. R., Stallcup, M. R., and Aswad, D. W. (2001). Methylation of histone H3 by coactivator-associated arginine methyltransferase 1. Biochemistry *40*, 5747–5756.

Shi, L., and Wu, J. (2009) Epigenetic regulation in mammalian preimplantation embryo development [Review]. Reprod. Biol. Endocrinol. *7*, 59, 133–144.

Strumpf, D., Mao, C. A., Yamanaka, Y., Ralston, A., Chawengsaksophak, K., Beck, F., and Rossant, J. (2005). Cdx2 is required for correct cell fate specification and differentiation of trophectoderm in the mouse blastocyst. Development *132*, 2093–2102.

Suwinska, A., Czolowska, R., Ozdzenski, W., and Tarkowski, A. K. (2008). Blastomeres of the mouse embryo lose totipotency after the fifth cleavage division: expression of Cdx2 and Oct4 and developmental potential of inner and outer blastomeres of 16- and 32-cell embryos. Dev. Biol. *322*, 133–144.

Thomas, F. C., Sheth, B., Eckert, J. J., Bazzoni, G., Dejana, E., and Fleming, T. P. (2004). Contribution of JAM-1 to epithelial differentiation and tight-junction biogenesis in the mouse preimplantation embryo. J. Cell Sci. *117*, 5599–5608.

Torres-Padilla, M. E., Parfitt, D. E., Kouzarides, T., and Zernicka-Goetz, M. (2007). Histone arginine methylation regulates pluripotency in the early mouse embryo. Nature *445*, 214–218.

Vinot, S., Le, T., Ohno, S., Pawson, T., Maro, B., and Louvet-Vallee, S. (2005). Asymmetric distribution of PAR proteins in the mouse embryo begins at the 8-cell stage during compaction. Dev. Biol. *282*, 307–319.

Wu, Q., Bruce, A. W., Jedrusik, A., Ellis, P. D., Andrews, R. M., Langford, C. F., Glover, D. M., and Zernicka-Goetz, M. (2009). CARM1 is required in ES cells to maintain pluripotency and resist differentiation. Stem Cells *27*, 2637–2645.

Vestweber, D., Gossler, A., Boller, K., and Kemler, R. (1987). Expression and distribution of cell adhesion molecule uvomorulin in mouse preimplantation embryos. Dev. Biol. *124*, 451–456.

Wysocka, J. (2006). Identifying novel proteins recognizing histone modifications using peptide pull-down assay. Methods *40*, 339–343.

Yadav, N., Lee, J., Kim, J., Shen, J., Hu, M. C., Aldaz, C. M., and Bedford, M. T. (2003). Specific protein methylation defects and gene expression perturbations in coactivator-associated arginine methyltransferase 1-deficient mice. Proc. Natl. Acad. Sci. USA. *100*, 6464–6468.

Zernicka-Goetz, M., Pines, J., McLean Hunter, S., Dixon, J. P., Siemering, K. R., Haseloff, J., and Evans, M. J. (1997). Following cell fate in the living mouse embryo. Development. *124*, 1133–1137.

Zernicka-Goetz, M., Morris, S. A., and Bruce, A. W. (2009). Making a firm decision: multifaceted regulation of cell fate in the early mouse embryo. Nat. Rev. Genet. *10*, 467–477.

Zhang, Y., and Reinberg, D. (2001). Transcription regulation by histone methylation: interplay between different covalent modifications of the core histone tails. Genes Dev. *15*, 2343–2360.